Tomographic ENA Imaging from Low-Earth Orbit

R. B. Sheldon

The University of Alabama in Huntsville

T. E. Fritz and H. E. Spence

Boston University Center for Space Physics

Abstract

With the immanent launch of IMAGE and TWINS, and the past successes of the ISEE, Geotail and POLAR energetic neutral atom (ENA) images, comes a tendency to perceive ENA imagers as primarily high-altitude instruments. However, the absolute flux of ENAs is far greater in low-earth orbit at 800km than any of the locations of the above mentioned satellites. This high flux, combined with the rapid orbital motion, permit tomographic inversion of the images received, for a true, three-dimensional image of the energetic particle population on these near-earth flux tubes. Since the ENA flux is a product of ion population and neutral atmosphere, an imaging satellite must also carry optical instruments that can ascertain the neutral densities so that absolute ion fluxes can be deconvolved. In addition, if the sattelite has ion instruments which sample *in situ* the same flux tube previously observed in ENAs, it is able to over-determine the data, so that instrumental errors can be removed to create an absolute density determination. We sketch out the valuable new observations and the potentially paradigm changing images available from this unique perspective, including tomographic views of magnetic substorms and storms, maps of the electric field along the flux tubes of the auroral acceleration region, and small-pitchangle, low-altitude extension of the ring current and plasma sheet, which can be imaged easily with high temporal and spatial resolution.

Introduction: The Significance of and Scientific Basis for Low Altitude Imaging

Two of the most important dynamic features of the magnetosphere are geomagnetic storms, characterized by ring current intensifications with Dst variations, and substorms, characterized by magnetotail reconfigurations with auroral electrojet variations and their related visible auroral manifestations. Each event is a global magnetospheric response to changes in the solar wind and interplanetary magnetic field. For the past thirty years, we have been limited in our ability to understand the global nature of these phenomena. While we have amassed a great volume of single-point, *in situ* measurements that provide the global picture in an average, static sense (space climatology), we have lacked an instantaneous view of large-spatial-scale magnetospheric dynamics (space weather). This lack of a global perspective has limited our analysis of the *in situ* measurements. In addition, the lack of these global data limit our ability to differentiate between various physical models that describe magnetic storms and substorms. These limitations include inadequate global knowledge of particle origins, loss processes, transport mechanisms and their time dependence.

Unfortunately, ions and magnetic fields are “invisible.” These quantities are dynamic and can only be measured when we fly through them with a spacecraft. Single point measurements thus cannot separate temporal from spatial variability, nor can they provide a global view. The novel approach of ENA imaging however gives us the global vision we need. Great progress has been made recently in ENA magnetospheric imaging. Beautiful images of energetic neutral atoms (ENAs) created by ion collisions with the Earth’s tenuous upper atmosphere have been collected by several satellites, including the POLAR satellite, which recently discovered (R. Sheldon) that both storms and substorms have strong and repeatable ENA signatures. These new global images demonstrate the feasibility and scientific usefulness of remote sensing to understand quantitatively the magnetospheric response to solar events [*Jorgensen et al.*(1997), *Henderson et al.*(1997),]. In the hypothetical low-Earth orbit mission, TENACIOUS (Tomographic ENA Comprehensive Ion and Optical University Satellite) a suite of instruments is proposed that can substantially increase our knowledge and insight into the magnetospheric responses by providing *in situ* measurements of particle fluxes and supporting optical emissions to complement ENA imaging. Ultimately, with this new knowledge, we will be able to better understand and predict the magnetic substorms and storms that energize and transport energetic particles in the geospace environment.

High-Altitude ENA Images

The power of ENA measurements from spacecraft has been amply demonstrated recently on orbit (ASTRID, POLAR, GEOTAIL) - but particularly so at high altitudes by the CEPPAD/IPS on the POLAR spacecraft. A schematic of how a high altitude imager remotely senses the ENAs produced by charge exchange between the geocorona and the energetic ions of the ring current is shown in Figure 1. This figure illustrates how a two dimensional image of the optically-thin ENA emissions can be formed from a single vantage point.

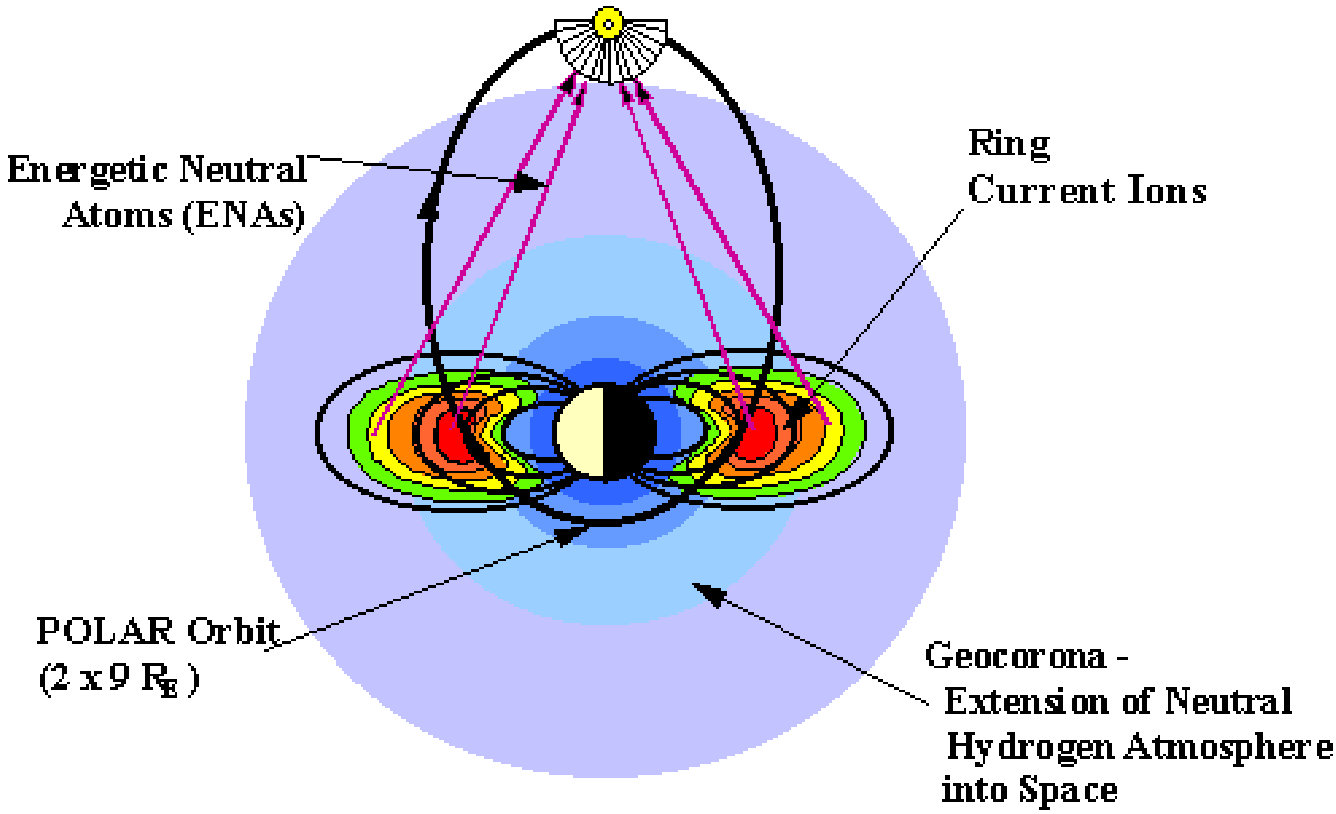

Figure 1. Schematic of Global Energetic Neutral Atom Imaging

From high apogee orbits, ENA images can be obtained on a global scale. However, ENA emissions are optically thin and involve the convolution of a three-dimensional neutral atmosphere with the ion density distributions, interacting with an energy-dependent charge exchange cross-section. Thus, data from a single ENA sensor provides a non-unique determination of the ion fluxes along the line-of-sight. Ideally, multiple measurements are required to obtain an unambiguous spatial distribution. The impending IMAGE and TWINS missions have taken the necessary first steps toward stereoscopic imaging of geospace with neutral atoms.

Yet not every ambiguity is removed. Although this stereoscopic view removes the two-dimensional ambiguity, it does not yet solve the separation of neutral from ion densities in the convolution. At best, it provides boundary conditions on the non-unique inversion. Worse yet, the low flux of ENAs requires long integration times, and therefore cannot resolve fine temporal changes, certainly not 10's of seconds, and possibly as poor as 10's of minutes. Therefore, as *Gruntman* [1997] points out in his excellent review article on ENA imaging, views from both the "outside looking in" (e.g., POLAR, IMAGE, TWINS) and from the "inside looking out" (e.g., TENACIOUS) are critically needed in order to extract the most meaningful physical information from the images. This need is driven by the fact that the highest spatial resolution and tomography can only be obtained from low altitudes where the optically thin emissions are the brightest.

Now if high time- and spatial-resolution images conveyed no new physics, the distinction we have drawn is moot. We argue, however, that there are several important magnetospheric processes only revealed by this low-altitude technique. We consider first the advantage of high geocoronal neutral densities, and second the advantage of high ENA flux.

High Geocoronal Densities

Since the dynamic magnetospheric regions (say, $L>5$) connect magnetically to low-altitudes at mid- to high-magnetic latitudes, the feet of the flux tubes threading the inner magnetotail connect to the ionosphere in regions where the geocoronal density is high. Suppose we are interested in pinpointing the ENA brightening associated with substorms as an indicator of the substorm initiation region [*Jorgensen et al.*(1997)]. Since the neutral atmosphere is so tenuous at $L>7$ in the equatorial plane, we do not observe equatorial ENA flux until the accelerated ions are within geosynchronous orbit. Thus the initiation region may be ENA invisible at the equator, purely because the production rate is so low. However, if the substorm ion injection is isotropic, as most measurements indicate, there will be a noticeable flux precipitating at low altitude, at the foot of the field line, where ENA production is most plentiful because of the higher geocoronal density. An instrument at low altitude, then, has the best chance of observing the substorm initiation region by observing the accelerated neutrals escaping from the flux tubes having precipitating flux.

Now the identification of which flux tube contains this flux requires high spatial resolution. A low altitude spacecraft will have the needed resolution that is impractical for a high altitude spacecraft. The problem is simply one of optics. Neutral particles cannot be focussed, so that pinhole type optics are the best that can be achieved. In such an arrangement, resolution is traded for sensitivity, so that a high altitude satellite can choose one or the other, but not both. This makes the required resolution inherently impractical. Attempts to identify the trajectory within the ENA imager and thereby overcome this optics limitation, say, by penetrating an ultrathin carbon foil such as in IMAGE/MENA, fail at the low, 1 keV/nucleon energies produced in substorms. Therefore only a low altitude ENA imager can make this measurement. Only a low altitude ENA imager has the capability of capturing the ion enhancements in a global picture of a substorm onset.

High ENA Fluxes

A second, related effect is that the ENA flux is bright, enabling a low altitude imager to capture significant counts in a short time period. The time resolution of such an imager can be less than 1 second. This is not just a bonus, but a necessity since the satellite is travelling 7 km/s. Were the flux not bright enough, a longer integration time would lead to a severely smeared picture. This satellite motion can also be used to our advantage, permitting an entire sequence of images of the same emission region but from lines-of-sight that are constantly changing. These two features allow for tomographic inversions to be performed, just the same way that the BU TERRIERS mission could provide tomographic 3-D images of the upper atmosphere and ionosphere from a low altitude satellite.

If we suppose that a substorm begins at a particular location in the near Earth geotail, then we would expect an arc of flux tubes on the night side of the Earth to brighten in ENA emission during the event. Mapping a flux tube from the ionosphere to the tail has always been a major uncertainty in magnetospheric physics, not the least of which is the uncertainty introduced by Birkeland currents near the Earth. The ability to map a flux tube, say, from 400 km to 3000 km by following a 3-D emission will certainly improve our magnetic field models, constrain the Birkeland currents, image the open/closed flux tube boundary, and as we describe below, determine the parallel potentials along the flux tube. All these measurements are done globally, which is a much stronger constraint on the models than single point measurements, such as rocket borne instruments. Only a low altitude ENA imager can make these measurements, resolving long standing differences concerning the auroral acceleration region.

Therefore if the technique is capable of imaging the auroral acceleration region and/or the substorm initiation region, it has the potential to resolve some long lasting disputes within the space physics community, and make important progress in magnetospheric science not possible with high altitude imagers.

Overarching Scientific Goals and Objectives

TENACIOUS can perform the following measurements with the stated goals (also outlined in Table):

- obtain high-energy-spectral resolution images of ENAs with excellent time resolution, broad spatial coverage and exceptional spatial resolution in three dimensions;
- obtain ultraviolet (UV) images of major neutral species with comparable time resolution and comparable or better spatial resolution than ENA images both for ENA inversions and to determine the response of the upper atmosphere to magnetic storms and substorms;
- obtain radial neutral density (geocoronal) profiles by performing limb scans of ENA bright objects and determining the multiple scattering coefficients;
- obtain multiple line-of-sight views of the ENA source regions along the short-period orbit to allow for true tomographic inversions of the low-altitude extension of magnetospheric particle populations and the auroral acceleration region (especially for $L < 6.6$ Re);
- provide data bases for comparison with data from other available satellites to permit stereo ENA views of the magnetosphere;
- obtain *in situ* measurement of the charged particle energy distribution in regions with UV and ENA images; our orbit permits portions of the imaged regions to be directly sampled and hence over-determine the deconvolution;
- observe the peak energy of the substorm ENA population, thereby constraining the models of substorm ion acceleration;
- quantitatively relate high spectral/spatial/temporal resolution ENA image intensities to global particle fluxes and their dynamics, both locally and remotely driven, thereby constraining models of substorm onset.

Table 1. Summary of Scientific Objectives

o Magnetospheric Structure and Ring Current Dynamics
- Convection boundaries, energization, and global electric fields from spectra
- Ring current growth, decay, and azimuthal asymmetries
- Radiation belt physics
o Substorms and Tail Dynamics
- Substorm-related energetic particle acceleration
- Plasma sheet thinning/expansion and Substorm onset timing and location
- Auroral zone plasma pressure gradients
o Geocoronal Physics
- Response of the geocorona to changing conditions
- Non-sphericity of source region
o Auroral Structure and Acceleration
- Imaging auroral arcs, current regions, and energetic ion in/outflow regions
- Measuring the parallel potentials through a double-layer structure along a given flux tube

Current State of Magnetospheric Imaging at High and Low Altitudes

Over the last many years, the increasing sophistication of ENA imagers has led to better empirical global views of the stormtime ring current region. Early results from the ISEE spacecraft [*Roelof et al.*(1985), *Roelof*(1987),] demonstrated the concept of quantitative use of ENA observations and ENA imaging. More recent results from the GEOTAIL spacecraft [*Lui et al.*(1996),] demonstrated the ability of ENA measurements to provide not only energy but also ring current composition. Even at low altitudes, ENA imaging studies have already amply demonstrated the power of these data, both from free-flying spacecraft, such as ASTRID measurements of the ring current [*Barabash et al.*(1997), *Brandt et al.*(1999),], and from rocket experiments, such as "Poleward Leap" measurements of auroral proton arcs [*Soraas and Aarsnes*(1996),].

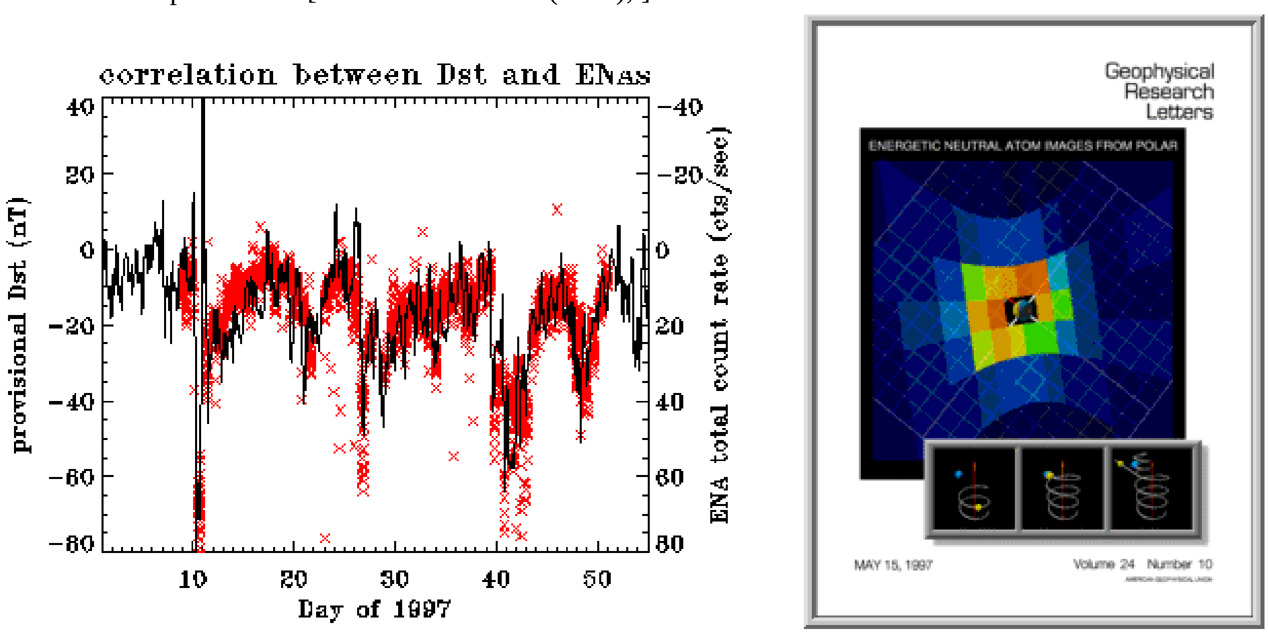

Figure 2. Correlation Between ENAs and Dst and Global Storm Imaging

The most contemporary high-altitude ENA results are from the POLAR spacecraft [*Jorgensen et al.*(1997), *Henderson et al.*(1997),] (see Figure 3) which emphasize the power of 2D imaging from a POLAR orbit and the ability to instantaneously image the entire ring current throughout a magnetic storm (see Figure 2). The POLAR ENA images permit, for example, the direct correlation of globally-integrated ENA images and the Dst index, and also are allowing us to track the stormtime injection process visually. The azimuthal asymmetry can be seen to evolve during a storm, reflecting the aggregate effects of ion drifts and the establishment and loss of the partial ring current. Despite the power of the POLAR data, the quantitative physical interpretation of the ENA images is confounded by their inherently low spatial resolution. The current pixel size projects to an area that is large in comparison to the neutral density scale height and the ion pressure gradient scale length in the ring current regions. This shortcoming represents an under-constrained data set from which it is difficult to extract unambiguous information on the populations that convolve to produce ENAs. This same problem will be encountered even by the much more capable IMAGE and TWINS imagers. By making complementary ENA images at low-altitude, the 3-D multiview and higher resolution TENACIOUS data can reduce these uncertainties and permit the important next level of quantitative analysis of stormtime injection both near the equator and possibly off the equator via parallel potentials.

For the TENACIOUS mission to succeed, we must observe the ENAs produced within geospace but from low-altitudes, a complementary vantage point to that of POLAR (the same as IMAGE and TWINS will provide). Do we have evidence that ENAs from these low-altitude regions will actually be observed? We have every expectation they should be. The equatorial distributions have fluxes near the loss cones–often comparable to the trapped fluxes–that will mirror at lower altitudes. These lower altitudes have much higher neutral densities, often by many orders of magnitude, so the commensurate rate of ENA production could be much higher. Furthermore, a low altitude spacecraft is considerably closer to this low-altitude source region so the emitted flux of ENAs should appear brighter. Such considerations have already been treated theoretically by several studies [*Orsini et al.*(1994), *Milillo et al.*(1996), *Roelof*(1997b), *Roelof*(1997a),] and these have shown that low-altitude imaging is not only viable but is highly desirable. Indeed, as noted above, both ASTRID and Poleward Leap observations demonstrate not only the existence of low-altitude ENAs but also their high intensity and also their scientific utility. Those are reviewed below. In addition, we present exciting new evidence from the long-running TIROS mission of considerable ENA fluxes detected at low altitude and their association with storms and substorms.

[*Barabash et al.*(1997)] used the ASTRID data to show a correlation, as in Figure 3, of the ENA flux measured from a low altitude orbit (1000 km) with Dst. Their instrument had a geometric factor of 2.5 $\times 10^{-3}$ cm^2-sr (somewhat smaller than that of the POLAR CEPPAD imager). Within the energy range of 26-37 keV, they observed ENA rates of 100 counts/second even during intervals of very weak ring activation (Dst $>$ -40 nT). These data were used to create maps of the ring current ions and used to do quantitative modeling of a small magnetic storm (Dst $\sim$ -80 nT) on 8 February 1995. Simulation results [*Brandt et al.*(1999),] and forward modeling revealed that during the main phase the ENAs seen at low altitude were consistent with a strong duskside source near the equator between L=4 to 8 centered at 19 MLT with a spread of about one hour of MLT. This is similar to the strong partial ring current peak observed in ENAs near the equator by POLAR.

[*Soraas and Aarsnes*(1996)] have used ENAs measured from the Poleward Leap sounding rocket to probe the structure of proton arcs in the auroral zone. They used a solid state detecting system with a geometrical factor of 4.3 x 10^{-2} cm^2-sr but were constrained to measure from altitudes below 454 km, in regions of multiple scattering in the higher density low altitudes atmosphere. At energies of 20-50 keV, they observe highly directional ENAs coming from a proton arc with rates approaching 1000 counts/second. Using these data, the study was able to observe ENAs in an arc during the expansion phase of a substorm and provide a regional map of the proton precipitation with excellent energy spectral resolution. The study showed a remarkably good agreement between the observed ENA emissions compared to a simple model of proton precipitation, even in this lower altitude regime where multiple scattering can have a blurring effect.

We note also in a study presently underway at Boston University [*Alothman and Fritz*(1998),], the discovery that even the NOAA TIROS spacecraft have been observing ENAs routinely from their 850 km polar orbit for decades. The TIROS orbit is at an altitude just midway between the rocket ENA measurements (<450 km) and the ASTRID measurements (1000 km). Like the Poleward Leap instrument, the TIROS energetic particle experiment is a simple solid state detecting system. However it possesses a higher energy threshold ($\sim$ 30 keV) than we would fly on TENACIOUS so that the rates it measures should be a lower limit approximation. TIROS measures ENAs at many hundred counts per second while in the polar caps looking back toward the auroral zone and ring current. Figure 4 shows a plot of TIROS ENAs, similar to Figure 3, demonstrating the relationship of ENA count rate to AL and Dst during a substorm and a magnetic storm.

In Figure 4, the solid colored crosses denote the average ENA rates measured by the TIROS spacecraft while in the polar caps looking back at the auroral zone and ring current regions. We can infer that these are ENAs by virtue of another detector looking toward the nadir which observed no discernible ion signal in the polar caps (squares). Over the course of several day periods, during the course of two magnetic storms in 1980, we can see that the ENA rate tracks both the Dst (black heavy line) and the AL indices (green line). Indeed, it is arguable that the ENA rates track the AL curve more closely than the Dst curve, suggesting that these are ENAs associated with higher latitude, auroral phenomenon, rather than lower latitude ring current phenomenon. From these powerful data, we therefore have every confidence that the unique TENACIOUS perspective from low altitudes, with high spectral-, temporal-, and spatial-resolution ENA images coupled with optical data, would provide critical new information on both storm and substorm studies.

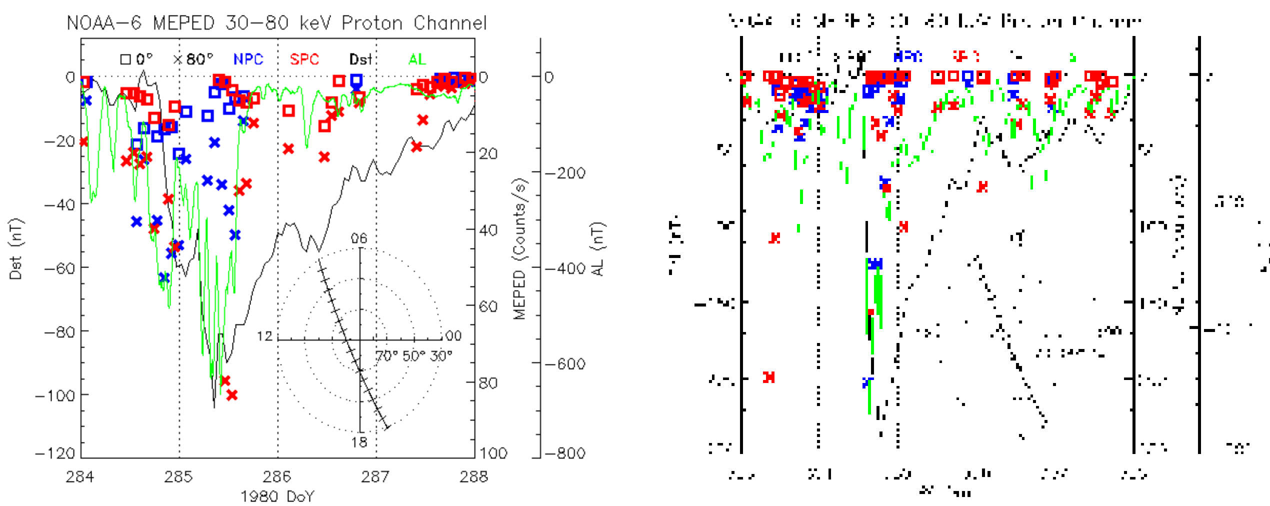

Figure 3. Correlation Between ENAs and Dst/AL From TIROS

New Applications of Low-Altitude Imaging

Geomagnetic Substorms

During a magnetospheric substorm, magnetic energy stored in the magnetotail lobes is converted, in part, to plasmasheet flow and inner magnetosphere plasma thermal energy. This energy conversion process is rapid, happening on the time scales of minutes. It produces large disturbances in the magnetotail magnetic fields and particles over broad spatial scales, perhaps starting as a highly-localized site of acceleration and thermalization and growing in scale over a short time. Because the magnetosphere is electrodynamically coupled, the energy dissipation from this reconfiguration is global, involving virtually all regions of the tail as well as the auroral ionosphere, an essential component of a substorm. The relative timing of substorm phenomena in the deep magnetotail (>40 Re), the mid-tail plasmasheet (20-40 Re), the near-tail plasmasheet (10-20 Re), the inner edge of the plasmasheet (5-10 Re), and the auroral ionosphere provide important information about the source of particle energization during substorms and the injection of hot plasma into geostationary altitudes. Statistical studies have established the average properties of substorm injections including their strength and radial and local time extent. However, the question remains as to how representative the average substorm is in terms of dynamics and spatial extent.

To be precise, two schools of thought have arisen concerning the trigger mechanism of a substorm. One school, the "near earth current disruption" (NECD) would place the trigger in the 6-15 Re region of the geotail. The other school, the "near earth neutral line" (NENL), would place the trigger 20-40 Re deep in the tail. It has been difficult for spacecraft to be in both places at the same time, and the chance occurrences of two spacecraft in the proper location is highly disputed. Thus the question as to the original trigger will most likely require a global, dynamic image of the entire region. That is, these questions can only be answered definitively by remotely observing the system globally and analyzing the *in situ* measurements in the context of the global evolution. TENACIOUS imagers would provide immediate insight into these decade old questions.

As noted previously, the promise of ENA imaging has been made clear recently by the POLAR spacecraft. POLAR has provided the first glimpse of the substorm injection region through global ENA imaging [*Henderson et al.*(1997), *Spence et al.*(1997),]. During the substorm life-cycle, ENA emissions are observed to first brighten weakly at the inner edge of the plasma sheet during a substorm growth phase, then intensify in a localized region near pre-midnight at substorm onset, and finally spread azimuthally (primarily to earlier local times) as the substorm enters the recovery phase. Thereafter the injected ions drift westward and decay while the associated ENA emissions subside. Simultaneous measurements at geostationary orbit confirm the tail stretching and subsequent ion injection while auroral images record the auroral arc brightenings and surge evolution. Despite the relative simplicity of the POLAR ENA measurements, significant qualitative understanding of the substorm injection process has already been made. The phenomena seen in the auroral zone and magnetotail are linked by the global images and the comprehensive view of spatial and temporal evolution allows us to test various substorm hypotheses.

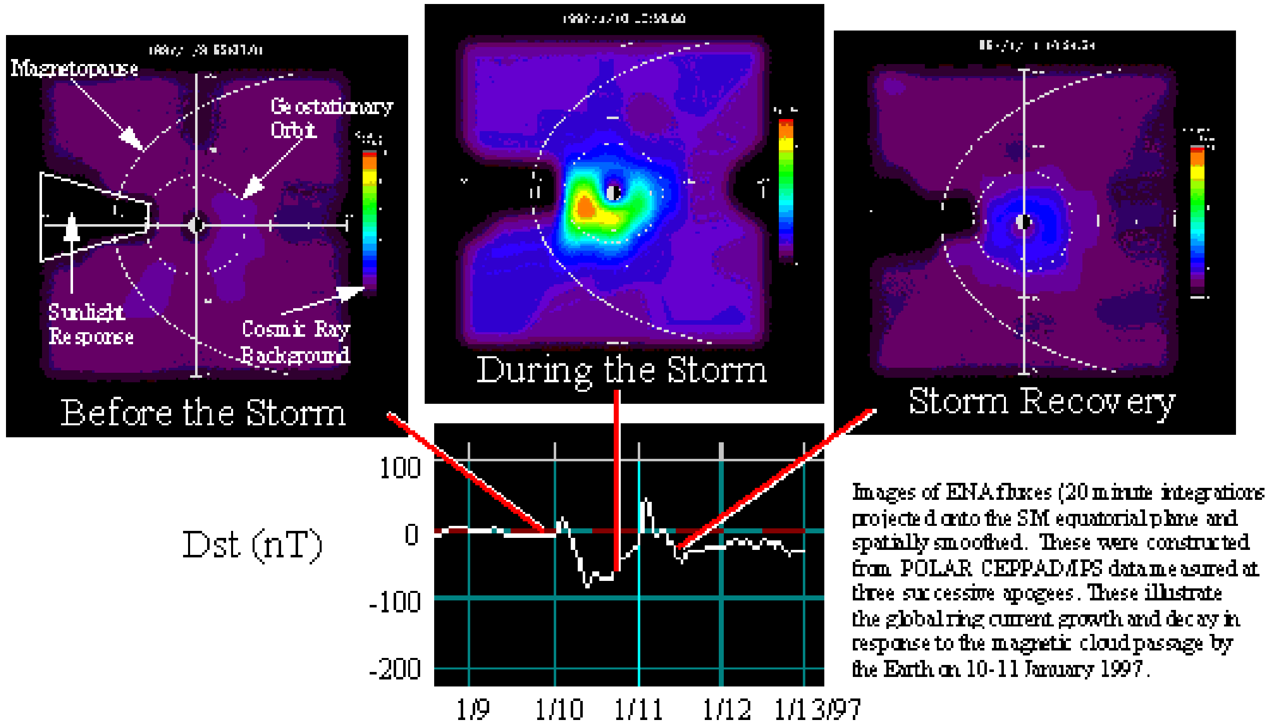

Figure 4. Global ENA Images from POLAR During a Moderate Magnetic Storm

However, these analyses are hampered by the inherent single point POLAR ENA measurements. Even with the multiple ENA data sets promised with IMAGE and TWINS, all these views are from the outside looking in and lack the ability to image with high spatial resolution the near-Earth extensions of these magnetospheric regions. For example, the middle to distant tail viewed at the magnetic equator will be virtually invisible in ENA, not primarily because there are no energetic ions, but rather owing to the very low geocoronal densities near the magnetic equator at such great distances. On the other hand, these same regions are visible from low altitudes–a small pitch-angle ion from the tail can charge-exchange in the high geocoronal densities near the Earth and thus be seen with a low-altitude ENA imager. The low-altitude, “inside-out” views provided by the TENACIOUS ENA imager would allow for substantially improved and routine observations of these regions and will complement nicely the global imaging provided by IMAGE and TWINS. Indeed, linking the high and low altitude signatures of substorms is extremely difficult with traditional methods and has led to great uncertainty in substorm model differentiation. A critical outstanding question to be answered is whether the substorm is initiated in a near-Earth current sheet disruption region that propagates tailward or is it initiated first at a near-Earth reconnection site whose effects propagate earthward? The next-generation ENA images should allow us to immediately establish the critical direction of propagation during a substorm and thus differentiate between competing substorm theories.

A second problem with POLAR (and potentially, IMAGE and TWINS) measurements, is that the energy spectrum of the ENA’s produced in substorms peaks at energies below threshold. The POLAR/IPS threshold was about 14-17 keV, which suggest that the actual peak is below 8 keV, and potentially, as low as 1 keV. If these ions have any substantial oxygen component, as they undoubtedly will at low altitude, the energy defect of typical solid state detectors (SSDs) or the equivalent “penetration energy” of Carbon-foils will completely mask the signal. Conversely, the energy may be too high for IMAGE/LENA to create a negative ion. Thus the TENACIOUS detector would have to blaze new ground in low energy ENA detection, using back-thinned charge coupled device (CCD’s) or ultra-violet (UV) blind multi-channel plates (MCP’s) to detect these substorm ENAs.

Magnetic Storms

A geomagnetic storm is characterized by the injection and energization of ions deep within the trapping region of the inner magnetosphere ($L<6.6$ Re). This trapped ion population decays to some resting state typically on the order of a few days. The storm time ion population is sufficiently energized such that its net guiding center drift leads to a strong enhancement of the westward-flowing, azimuthal ring current. The strong current near the magnetic equator between 2 and 6 Re depresses the Earth's surface magnetic field which defines the classic magnetic storm index, Dst. Early studies demonstrated the relationship between the energy content of the ring current and the strength of Dst as well as the large azimuthal asymmetries that can arise during the injection process (see Figure 2). Kinetic particle models rather than MHD models of the ring current are necessary owing to the large gyroradii of the pressure-bearing ions. Such models have evolved over the last twenty years but all depend on the specification of initial injected particle populations and evolving electric and magnetic fields that the particles react to during a storm cycle. These models have provided a theoretical view of the global system but until recently, have had relatively little data to constrain and test our understanding of the physics of storm injection. Most comparisons have been done with one or at most a few satellites traversing only portions of the volume important for the storm time development.

With POLAR, the growth and decay of the energetic ion population during a magnetic storm was directly tracked on a global scale for the first time using ENAs. The high geometric factor, excellent energy resolution, and capable spatial resolution of the POLAR ENA imager permit us to create global images of the ring current at high time resolution (on the order of several spacecraft spins or about one minute). An example of one such sequence of ENA images from POLAR is shown in Figure 2 during a magnetic storm in January 1997. This spatially-smoothed image shows the emissions mapped to the symmetry plane of the magnetic equator. A clear rise and fall and large local time asymmetry of the ENA flux is apparent. The partial ring current is clearly seen as fresh ions during a storm surge are injected deep into the trapping region and then drift westward owing to gradient-curvature effects; there is even evidence of ionospheric extraction of energetic ions during the main phase [*Sheldon and Spence*(1998), *Sheldon et al.*(1998),] of another storm in 1996. These ions carry an azimuthally-localized current that is seen on the ground as an asymmetric ground magnetic disturbance in local time. However, from the ground there is no clear way to know the radial or azimuthal distribution of current. Presently, only a crude asymmetry index called ASY is ever routinely produced. On the other hand, our POLAR images provide immediate global context for the analysis of point measurements within the globally imaged region. In one image, we see the local time, radial, and spectral distribution of the ring current ions and can track them in time at relatively high time resolution. These data are allowing us to test our models of electric field penetration and the complex particle accelerations during storm main phase and recovery.

Although high-altitude observations, such as IMAGE and TWINS, will permit excellent azimuthal reconstruction of the ring current, and hence the derivation of Dst from a first-order fit of the Fourier components, they do not perform as well in determining the pitch-angle dependence. This dependence can best be estimated by comparing the brightness at low altitudes with the brightness at equatorial altitudes along a single flux tube. Recent work, [*Sheldon et al.*(1998)] suggest that the most rapid decrease and recovery of Dst during truly large storms ($|\mathrm{Dst}| > 200$) may be due to very small pitchangle ions accelerated out of the ionosphere. By geometrical considerations, one can show that high-altitude imagers would have great difficulty seeing these ions at the equator, and insufficient resolution to resolve their flux tubes in the low-altitude loss cones. Only a low-altitude satellite could resolve how much, if any, Dst was due to direct ionospheric injection.

Auroral Acceleration

The NASA Small Explorer, FAST, has shown that the auroral zone is a region of complexity with interesting microphysics coupling to macroscale phenomenon. Part of the auroral puzzle is the distribution in space and time of auroral arcs. While FAST can make very rapid measurements, it is still limited in its ability to unravel spatial versus temporal variations. The bulk of auroral energies are below the SSD or C-foil instrument threshold, requiring the new technology to cover the energy range (1>¿ E $>$ 15 keV) however, both TIROS and POLAR data indicate that the auroral arc ENA's extend up to at least 40 keV. Therefore, TENACIOUS would have the chance of revealing the structures associated with proton aurora on a macroscopic scale. Owing to the spacecraft motion, we would then fly through the structure, possibly coincidentally, and thus be able to make excellent progress in unfolding the surrounding ion fluxes for the first time, with tomographic inversion techniques. As FAST has revealed, TENACIOUS would have the exciting possibility to image as a function of neutral atom energy two major auroral acceleration regions to complement classical optical images: the upward-accelerated ions associated with traditional auroral arc regions (from which auroral arc electric field structure may be inferred in 3D; and the so-called "black aurora" regions characterized by downward-going hot magnetospheric ions that neutralize at the feet of auroral field lines.

Radiation Belt

The mechanisms that form and accelerate the radiation belt particles can be different from the ring current. For example, both the CRAND source and the March 1991 solar wind shock produce radiation belt enhancements in a far different manner than the radial diffusion and adiabatic energization that forms the quiet time ring current. If the radiation belt ions are adiabatically transported to their low-L, high-B location, then one can confidently predict that the "source region" for the radiation belts has lower energy ions that are reduced by the ratio of magnetic field strengths, B_{source}/B_{belt}. Several regions have been proposed as sources of these ions, including the tail, the cusp and the boundary layer/ magnetosheath. None of these regions have high enough geocoronal densities to produce much ENA flux, but if they are mapped into the loss cone at low altitudes, a substantial ENA flux would result. The low altitude orbit of TENACIOUS, then, is the only place where these putative source populations could be remotely sensed. Therefore it is of great interest to spectrally resolve ENA's arising from high latitudes and differing MLT, for then we may be able to map the precursors to a radiation belt enhancement and resolve their sources.

Geocoronal Science

As powerful as the ENA measurements are, they do not return the source ion distributions without deconvolving the densities of the neutral, electron-donor background gas. On this basis alone, a measurement of the geocoronal density is essential, including not only [H], but also [He] and [O] at low altitudes. We accomplish this task by using spectroscopic tomographic inversion methods pioneered by TERRIERS, and applied to the EUV sunlight scattered by these species described later in Section D.2a. In addition to these neutral gases which form a purely gravitationally bound atmosphere, both He^+ and O^+ are conceivably important electron donors for ENAs whose densities would track the magnetically confined plasmasphere. [*Sheldon and Hamilton*(1993)] has shown that He and He^+ electron donor cross sections may actually dominate over H for select species and energy of ENAs. TENACIOUS would have the ability to track photometrically the three most abundant neutral gases [H], [He], and [O], as well as the most important plasma species [O^+] (excluding [H^+] which is photometrically invisible). These geocoronal measurements will complement those being made from high altitudes with advantages similar to those described for the ENA measurements.

Finally, the geocorona is an extension of the upper atmosphere that causes satellite drag, which has high variability both annually and during the solar cycle. It should be noted that the scale height of the geocorona varies most rapidly at low altitude precisely where TENACIOUS would have the best resolution. Thus, TENACIOUS is uniquely suited to providing a 3-D, time variable, dynamic geocoronal model.

Science Implementation

We can achieve the scientific goals and objectives outlined above with optimized instrumentation on TENACIOUS. The instrumentation described below either has proven spaceflight heritage or is based, with low- or little modification, on hardware previously developed for NASA missions. The instrumentation includes an Imaging Energetic Particle Sensor, IEPS (for energetic protons, neutral atoms, and energetic electrons), and a pair of Tomographic Extreme-UltraViolet Spectrometers, TESS (for geocoronal imaging) each tuned either for daytime or nighttime observations. We refer the interested reader to the TERRIERS satellite description for TESS, and POLAR satellite description for IPS. In this table we compare the TENACIOUS instrumentation with contemporaneous ENA telescopes.

Table 2. TENACIOUS ENA Imager Compared with Complementary Imagers

MISSION	TENACIOUS	IMAGE	TWINS	POLAR
Mission Type	UNEX	MIDEX	MOO	ISTP
ENA Instrument	IEPS	L/M/HENA	MENA	IPS
Global Imaging	regional	yes	yes	yes
Energy Range (keV)	15–400	10–200	1 – 100	15-1500
Energy Resolution (ΔE/E)	0.15	0.7	0.4	0.15
Number of Energy Bins	8	4		16
Angular Resolution (°)	12 x 20	4 x 6	4 x 4	12 x 20
Typ. Projected Spatial Res.(Re)	0.03x0.05	0.5 x 0.75	0.5 x0.5	1.9 x 3.2
Typ. Temporal Res. (sec)	10	300	60	96
Typ. pixel dimension (mm)	2.0 x 3.5	1.5 x 1.5		1.5 x 3.0
Geom. Fact./pixel (cm^2-sr)	$5x10^{-3}$		$1.4x10^{-3}$	$3x10^{-3}$

Optimal altitude determination

We note that low Earth orbit is a novel, and in many ways an optimal, location to perform magnetospheric neutral atom imaging. We have noted the advantages previously. One concern is the multiple scattering of ENAs that can occur in the denser regions of the atmosphere. This question has been treated theoretically and shown that altitudes above 850 kilometers are nearly scatter-free. Altitudes at 1000 kilometers or higher are optimal from an ENA point of view, but higher altitudes introduce radiation damage effects to sensor electronics from the inner edge of the radiation belt and the inward bulge of the south Atlantic anomaly. *Soraas and Arsnes* [1996] showed from their rocket data that even at 450 kilometers the effects of scattering were still surprisingly minimal. Indeed, *Gruntman* [1997] alluded to the fact that problems attributed to multiple scattering have probably been overestimated based on simple theory. Therefore we target an apogee altitude for TENACIOUS at 1000 km to be well within a single encounter (optically thin) ENA regime. Anything above 850 km would be acceptable so we are actually very insensitive to exact altitude. Indeed, by choosing an elliptical orbit with perigee at 400 km and apogee at 1000 km, one could model the radial dependence of multiple scattering, as well as provide an *in situ* independent measure of geocoronal scale heights at these critical radii. With five measurements of the three quantities: ions, neutrals and ENAs, the TENACIOUS mission would put stringent constraints on all models of low-altitude fluxes.

Summary

Therefore a low-altitude ENA imager not only has the opportunity of measuring the global dynamics of storms and substorms, but also the absolute fluxes of ions and neutrals in this critical "exobase" region of the collisional geocorona. These measurements would then have the potential of resolving both long-standing debates within the magnetospheric community, and improving by an order of magnitude, the empirical models of the geocoronal exobase.

References

Alothman, M. J. and T. A. Fritz. Investigation of cusp energetic particle events signature in the high latitude trapping boundary. *EOS Trans. Suppl.*, *79*(17), S297, 1998.

Barabash, S., P. C:son Brandt, O. Norberg, R. Lundin, E. C. Roelof, C. J. Chase, B. H. Mauk, and H. Koskinnen. Energetic neutral atom imaging by the ASTRID microsatellite. *Adv. Space Res.*, 1997.

Brandt, P. C:Son, S. Barabash, O. Norberg, R. Lundin, E. C. Roelof, C. J. Chase, B. H. Mauk, and M. Thomsen. Ena imaging from the Swedish microsatellite ASTRID during the magnetic storm of 8 February 1995. *Adv. Space Res.*, 1999.

Gruntman, M. Energetic neutral atom imaging of space plasmas. *Rev. Sci. Inst.*, *68*, 3617–3656, 1997.

Henderson, M., G. Reeves, A. Jorgenson, H. Spence, R. Sheldon, B. Blake, and J. Fennell. First energetic neutral atom images from POLAR/CEPPAD/IPS. *Geophys. Res. Lett.*, *24*, 1167–1170, 1997.

Jorgensen, A. M., H. E. Spence, M. G. Henderson, G. D. Reeves, M. Sugiura, and T. Kamei. Global energetic neutral atom (ENA) measurements and their associeation with the Dst index. *Geophys. Res. Lett.*, *24*, 1167–1170, 1997.

Lui, A. T. Y., D. J. Williams, E. C. Roelof, R. W. McEntire, and D. G. Mitchell. First composition measurements of energetic neutral atoms. *Geophys. Res. Lett.*, *23*, 2641–2644, 1996.

Milillo, A., S. Orsini, I. A. Daglis, and G. Bellucci. Low-altitude energetic neutral atoms imaging of the inner magnetosphere: A geometrical method to identify the energetic neutral atoms contributions from different magnetospheric regions. *J. Geophys. Res.*, *101*, 27123, 1996.

Orsini, S., I. A. Daglis, M. Candidi, K. Hsieh, S. Livi, and B. Wilken. Model calculation of energetic neutral atoms precipitation at low altitudes. *J. Geophys. Res.*, *99*, 13489, 1994.

Roelof, E. C., D. G. Mitchell, and D. J. Williams. Energetic neutral atoms (E$\sim$50keV from the ring current: IMPS 7/8 and ISEE 1. *J. Geophys. Res.*, *90*, 10991, 1985.

Roelof, E. C. Energetic neutral atom image of a storm-time ring current. *Geophys. Res. Lett.*, *14*, 652–655, 1987.

Roelof, E. C. ENA emission from nearly mirroring magnetospheric ions interacting with the exosphere. *Adv. Space Res.*, *20*, 361, 1997a.

Roelof, E. C. Energetic neutral atom imaging of magnetospheric ions from high and low altitude spacecraft. *Adv. Space Res.*, *20*, 341, 1997b.

Sheldon, R. B. and D. C. Hamilton. Ion transport and loss in the earth's quiet ring current 1. data and standard model. *J. Geophys. Res.*, *98*, 13,491–13,508, 1993.

Sheldon, R. B. and H. E. Spence. A new magnetic storm model. In J. Horwitz, editor, *Geospace Mass and Energy Flow: Results from the International Solar-Terrestrial Physics Program*, pages 349–354, Washington, D.C., 1998. AGU.

Sheldon, R. B., H. E. Spence, and J. F. Fennell. Observation of 40 kev field-aligned ion beams. *Geophys. Res. Lett.*, *25*, 1617–1620, 1998.

Soraas, F. and K. Aarsnes. Observations of ENA in and near a proton arc. *Geophys. Res. Lett.*, *23*, 2959–2962, 1996.

Spence, H. E., A. M. Jorgensen, T. A. Fritz, R. B. Sheldon, M. G. Henderson, G. D. Reeves, J. B. Blake, J. F. Fennell, and D. N. Baker. The substorm injection revealed: global ENA images and simultaneous multipoint observations of the substorm lifecycle. *EOS Trans. Suppl.*, page F612, 1997.

UAH Physics Dept OB201, Huntsville AL 35899

This preprint was prepared with AGU's LaTeX macros v4. File jatp1 formatted October 25, 1999.